'SUPER CAMP': A RESEARCH PROJECT TO INVESTIGATE THE POLAR MIDDLE ATMOSPHERE IN SUMMER WITH ROCKET LAUNCHES FROM 65°–80°N

E Kopp[1], C R Philbrick[2], G E Thomas[3], & G Witt[4]

[1] *Physikalisches Institut, University of Bern, Switzerland*
[2] *Air Force Geophysical Laboratory, Bedford, USA*
[3] *Laboratory for Atmospheric & Space Physics, University of Colorado, Boulder, USA*
[4] *Meteorological Office, University of Stockholm, Sweden*

ABSTRACT

An international campaign "Super CAMP" (CAMP: Cold Arctic Mesopause Project) is proposed for summer 1988 which will be focussed to study the structure and dynamics of the middle atmosphere (50-150 km) above the north polar region. The polar summer mesosphere is characterized by the presence of the thin, persistent and dense clouds at altitudes 82-86 km north of 70°N latitude. The polar mesospheric cloud layer (PMC), as observed from the SME satellite, is the source of ice particles which are visible from ground as Noctilucent Clouds (NLC) in summer at high latitudes (>70°N).

Super CAMP should concentrate on following goals:

- Measurements of water vapor, ozone and temperature and its variability as a function of time, geomagnetic and meteor shower activity.
- Formation, particle size and density, transport and life time of NLC particles.
- Dynamics and temperature and their effects on ice particle growths and the distribution of minor constituents including the ionospheric plasma.
- Electric fields, charged aerosols, massive positive and negative ions in the vicinity of NLC.

In situ measurements from rockets, grouped in 2-3 salvos should be supported by ground, airborne and satellite remote sensing experiments in the latitude region 60-80°N. Rocket launchings from Nord, Greenland (81.5°N) and/or Thule, Greenland (76.6°N) would offer a study of the mesosphere where NLC particles originate.

Keywords: Middle Atmosphere, Summer Mesosphere, Polar Region, Rocket Campaign.

1. INTRODUCTION

The cold arctic mesopause in summer has been a subject of interest since the time when noctilucent cloud observations located these clouds at an altitude of 80-87 km (Jesse, 1896). Models by Murgatroyd (1957), and Murgatroyd and Singleton (1961) have indicated the temperature minimum of the atmosphere at the high latitude summer mesopause. In their calculation the summer high latitude is cooled by ascending air between 50-80 km with ascent speeds of 1 cm/s. Based on the large seasonal temperature variation of the arctic mesopause Hesstvedt (1961) concluded that the for-

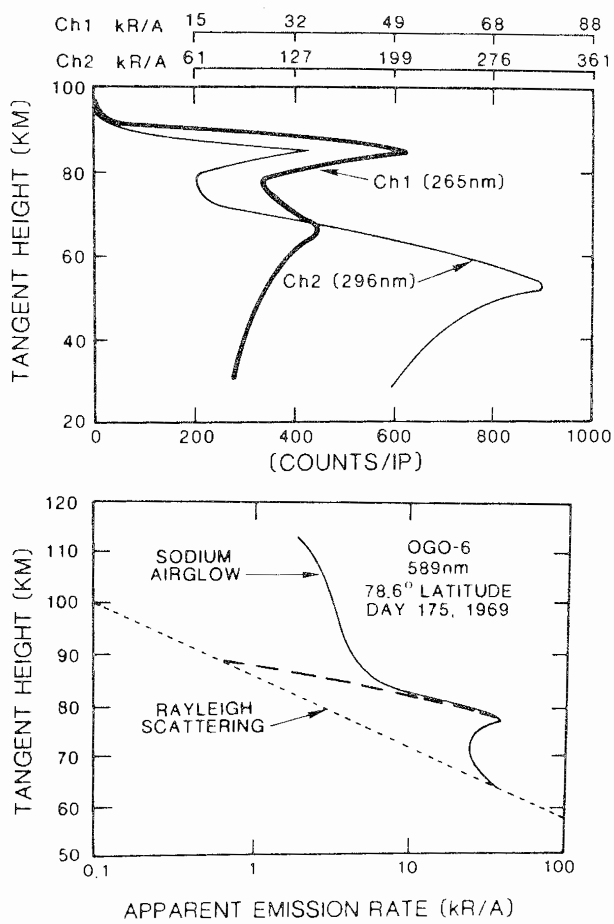

Fig. 1. Limb profiles of PMC taken by the SME ultraviolet spectrometer (upper panel) and the Ogo-6 visible light photometer (lower panel). The ordinate in both figures is the minimum ray height of the line of sight. The lower portions of both data sets are due to scattering from air molecules in the mesosphere. The lower peaks in the UV data are due to O_3 absorption. (Thomas and McKay, 1985)

Proceedings of the 7th ESA Symposium on European Rocket & Balloon Programmes and Related Research, Loen, Norway, 5–11 May 1985 (ESA SP-229, July 1985).

mation of ice crystals at the mesopause is the cause of formation of NLC's. In situ temperature measurements by Theon et al. (1967) with NLC's above Pt. Barrow (71°N) using the grenade technique have revealed temperatures below 140°K at altitudes 83-88 km in the period Aug 7/9 1965. The wave like deformation seen in noctilucent cloud with patterns was first associated with gravity waves by Hines (1968). The horizontal wavelengths of NLC bands are typically 30-80 km. Hines has argued that mesospheric gravity waves originate at tropospheric levels. Recent interpretation by Fritts et al. (1984) of Poker Flat MST radar data is more in favor for tidal waves in the summer high latitude mesosphere. The change of brightness of the scattered light from ice particles is interpreted as due to small changes in particle radii, brought on by variations in temperature and vertical wind velocity due to gravity and/or tidal waves.

A dense and persistent cloud layer at 80-85 km located over the summer geographic pole was discovered by Donahue et al. (1972) from satellite photometric measurements at visible wavelengths. The Ultraviolet Spectrometer Experiment on the Solar Mesosphere Explorer (SME) satellite obtained scattered light measurements (cf. Fig. 1) from these clouds, named Polar Mesospheric Clouds (PMC), in two UV-wavelength ranges over five seasons (Thomas, 1984). The inferred size of ice particles by Thomas and McKay (1985) in PMC's gave maximum particle radii of 70 nm and a mean particle radius range of 40-60 nm. The PMC thickness appears to be less than 5 km, the particle densities are several hundred cm^{-3} (based on a monodispose assumption) and the inferred water content generally consistent with the expected water vapor mixing rates (3-5ppmv).

An analysis of the summertime windfield between 80-93 km over Poker Flat, Alaska, by Carter and Balsley (1982), using the MST-radar technique, gives a consistent wind situation from year to year. The mean zonal wind velocities are typically 20-40 m/s in westward direction. The mean meridional wind has a velocity of 10-20 m/s southward. The meridional wind is in good agreement with other wind measurements using the doppler radar, meteor radar or particle reflection technique as reviewed by Nastrom et al. (1982).

The formation of NLC-particles by ion nucleation and water condensation and/or water nucleation on dust and coagulation of ice crystals requires a time scale of the order of 12-24 hours (Turco et al., 1982). Visible NLC ice particles, observed at twilight from ground at latitudes around 60°, are thus transported southward and westward from the polar cap region (75-85°), the region of PMC's, while growing to their final size.

2. PREVIOUS COORDINATED ROCKET CAMPAIGNS

In situ measurements of the cold arctic mesopause were made in three coordinated sounding rocket campaigns summarized in Table 1 from the rocket ranges Esrange (Kiruna) and Poker Flat (Alaska). Both ranges are located in the auroral zone. The rocket payloads had instruments to measure temperature, density, horizontal winds, electron and total ion densities, ion and neutral composition, and the energetic particle flux. Several passive and active optical experiments were used to measure atomic oxygen, the scattered light from NLC-particles and the light of Lyman-α and Schumann-Runge band. The CAMP (1982) and the STATE (1983) campaigns had supporting measurements from ground (Eiscat, MST-radar, optical, and meteorwind radar measurements) from airplane (NLC-detection, microwave experiments for H_2O densities) and from satellites (SME and Nimbus 7).

Table 1: Coordinated Rocket Campaigns at the Summer High Latitude

Date	Name	Salvos	Reference
1978 July/Aug Kiruna	NLC-Campaign	2 Salvos 8 rockets	Björn et al. (1985)
1982 Aug Kiruna	CAMP	2 Salvos 10 rockets	Björn (1984) Kopp et al. (1985)
1983 June Poker Flat	STATE	3 Salvos 7 rockets	Philbrick et al. (1984)

An active falling sphere of 25 cm in diameter with a triaxial piezoelectric accelerometer (Philbrick et al. 1978) was ejected from the TAD payload in salvo A during CAMP, 3/4 Aug 1982. This technique gave a unique capability for measuring temperature and horizontal wind profiles with a resolution of about 100 m. Three distinct temperature minima were measured at 83.5, 89.4 and 93.6 km with temperatures as low as 139°K, 119°K, and 111°K respectiveley (Philbrick et al. 1984). These temperatures are significantly lower than any which have been measured previously. The zonal wind profile revealed a wave like pattern, with a vertical wavelength of $\lambda_z \sim$ 7-8 km and a mean westward wind velocity increasing with altitude from 80 m/s at 80 km to 90 m/s at 90 km. The zonal wind reversal took place at an altitude of 95 km. The unique combination of temperature and horizontal wind velocity measurements can be used to determine regions of dynamic instabilities based on the Richardson numbers:

$$Ri = \frac{N_B^2}{\left(\frac{\partial u}{\partial z}\right)^2}$$

$$N_B^2 = -g \left[\frac{1}{\rho}\frac{\partial \rho}{\partial z} + \frac{g}{\gamma R T} \right], \text{ Brunt Väisäla frequency}$$

u = horizontal wind velocity.

The Richardson numbers from the CAMP wind and temperature measurements are given in Fig. 2. The regions with Ri<1/4 indicate dynamically unstable situations around 75 km, 79 km, 86.2 km, 89 km and 92.5 km altitude. All these regions are clearly located in the middle to upper mesosphere. The location of the turbulent layers are in good agreement with the summer measurements above Poker Flat (Balsley et al., 1983) and Andenes (Rüster, 1985) as obtained from the MST-radar.

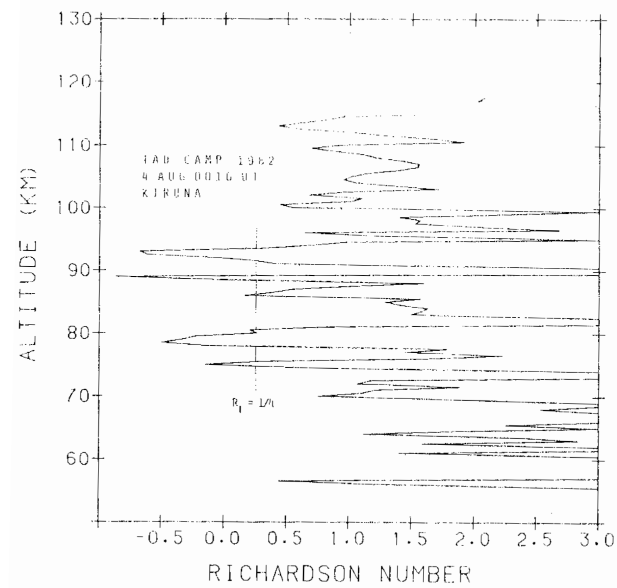

Fig. 2. Richardson numbers inferred from temperatures and horizontal wind velocity measurements during CAMP, in salvo A, on Aug 3/4, 1982 by the piezoelectric accelerometer technique. The regions with Ri<1/4 indicate dynamically unstable layers.

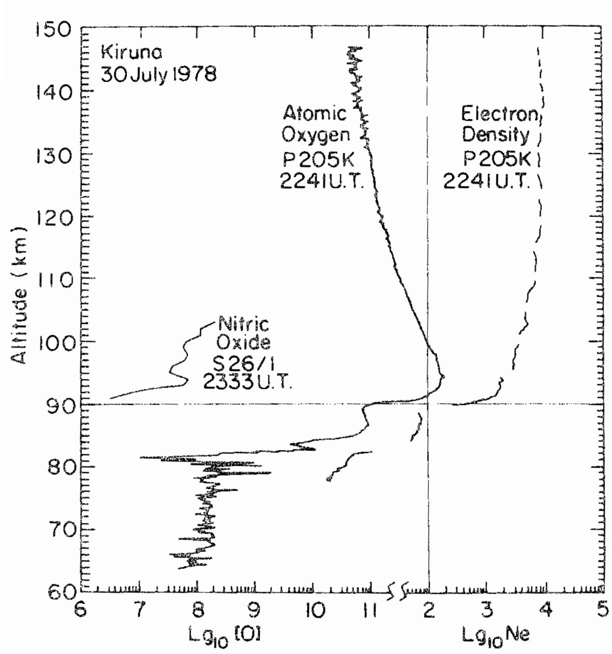

Fig. 3. Measured density profiles of atomic oxygen electrons and inferred density profile of nitric oxide derived from positive ion composition. Measurements were taken during the NLC campaign 1978 above Kiruna.

The high measurement rates used on the electron density probes in the STATE campaign 1983, gave clear evidence of an increase of turbulence in the height region where the MST radar echoes had maximum signal to noise ratios at altitudes above 84 km and 88 km respectively (Philbrick et al., 1984). At altitudes below 100 km the motion of electrons and ions is controlled by the neutral gas due to the high collision frequency.

The atomic oxygen and nitric oxide density in the NLC campaign 1978 (cf. Fig. 3) and in CAMP decreased at least one order of magnitude at altitudes below 90 km. The low mesospheric O and NO densities in summer reflect a situation with a dynamically controlled region above 90 km and a chemically controlled region below 90 km. The thin layers of dynamic instabilities found from the temperature and wind measurements also appear in the atomic oxygen and electron profiles as seen in Fig. 3 at an altitude of 87-89 km, in the 1978 NLC campaign. The atomic oxygen profiles of CAMP have similar zones where their density is affected by local turbulence. Both atomic oxygen density profiles measured in the NLC campaigns 1978 and 1982 (CAMP) have a characteristic depression with a density decrease of a factor of two at 81-83 km, the height where visible NLC clouds have been observed. It is, however, not yet clear, if this depression is caused by additional loss of atomic oxygen with odd hydrogen compounds or through reactions on the water ice surface.

The temperature profile from the active falling sphere experiment can be used to derive the water vapor saturation ratio S relative to a flat surface of ice or water. The altitude profile of the ratio S in Fig. 4 reveals three regions of supersaturation during CAMP 1982, with high S values of 100 at 89 km, and 70 at 94 km.

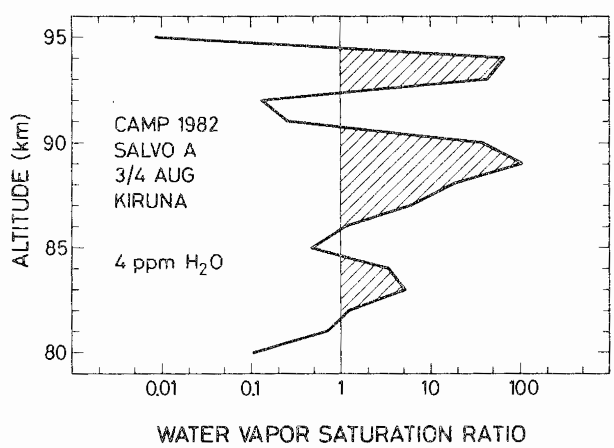

Fig. 4. Water vapor saturation ratio S relative to a flat surface of ice or water, derived from the temperature measurement during CAMP in salvo A, on Aug 3/4, 1982, by the piezoelectric accelerometer technique.

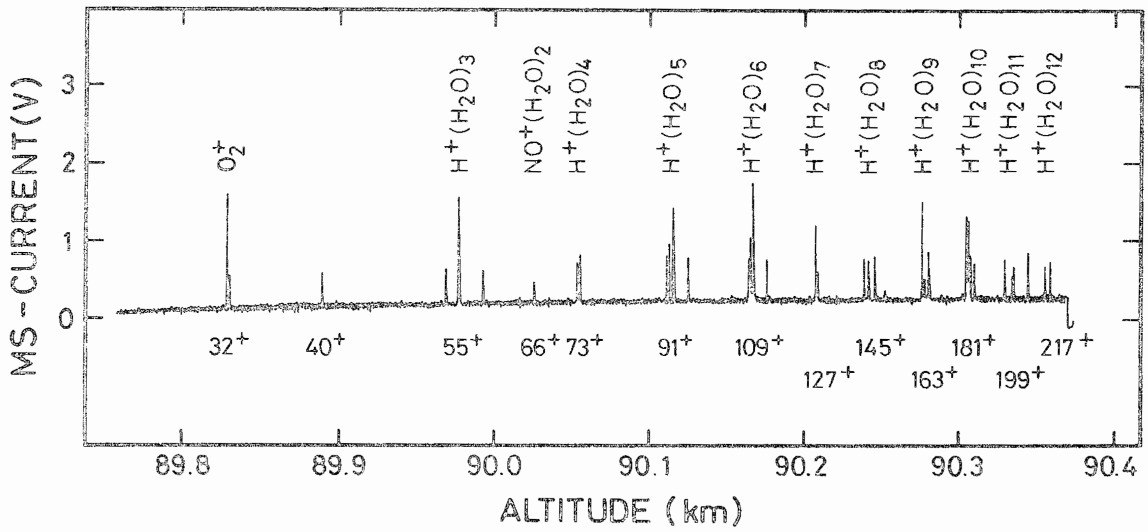

Fig. 5. Positive ion spectrum obtained by the magnetic ion mass spectrometer at 90 km on ascent of rocket flight S 26/1 above Kiruna, on July 30, 1978. (see e.g. Björn et al., 1985).

According to the NLC model by Turco et al. (1982) high water saturation values in the upper mesosphere will favor the mechanism of ion nucleation and condensation of water vapor. A region of ion nucleation was detected by the ion mass spectrometers of the University of Bern and the Max-Planck-Institut of Kernphysik in Heidelberg (Kopp et al., 1985, Björn and Arnold 1981) in the NLC campaign 1978. Fig. 5 shows the positive ion spectrum from this region at an altitude of 90.0-90.4 km with a flat density spectrum of proton hydrates up to $H^+(H_2O)_{12}$, a region with a rapid build up of large ions. Although this region of ion nucleation was measured above Kiruna the westward and southward air transport over the summer pole in the mesosphere suggests that the NLC ice particles are generally formed at higher latitude (> 70°) over the polar cap. A built-up time for NLC particles from large cluster ions is 12-24 h. Within one day these growing ice particles will fall downward and drift westward and southward from the polar cap region towards the NLC regions at latitudes 55-70°.

The main scientific results from the three high latitude summer campaigns listed in Table 1 can be summarized as:

- Three distinct temperature minima were measured in the CAMP campaign at 83.6 km, 89.4 km and 93.6 km with temperature values as low as 139°K, 119°K, and 111°K, respectively.

- The mean zonal wind velocity of salvo A in CAMP was 80 m/s westward, and the mean meridional wind velocity 40 m/s southward.

- The amplitude of the vertical wind velocity w' measured by EISCAT above Kiruna was 15 m/s. The corresponding gravity or tidal wave parameters were: w'∿ 15 m/s, u'∿ 30 m/s, λ_z∿ 10 km, λ_x∿ 60 km and the wave period ∿ 40 min.

- Superadiabatic lapse rates were responsible for the formation of dynamically unstable layers in the mesosphere during CAMP.

- A thin layer of heavy proton hydrates $H^+(H_2O)_n$ (mass range: 55-350u) was measured at 90-90.5 km altitude above Kiruna in the 1978 NLC-campaign. This region gives evidence for the ion nucleation mechanism.

- The density profiles of atomic oxygen and nitric oxide revealed two regions, the region above 90 km which is dynamically controlled and the region below 90 km with considerably lower densities ([O]∿ $10^{10}cm^{-3}$, [NO]∿$5x10^6cm^{-3}$) and the dominance of chemical loss over the turbulent mixing.

- The density profiles of electrons and atomic oxygen are affected in regions of instabilities and NLC's.

- The wind field of the summer polar mesosphere as observed by MST-radars and meteor wind radars has a westward zonal mean wind and a southward mean meridional wind component.

- The water vapor mixing ratio inferred from positive ion composition was around 3 ppmv in the altitude 80-90 km on Aug 13, 1978 above Kiruna.

3. ANNUAL AND SEASONAL VARIATIONS OF NLC and PMC

A recent report by Gadsden (1985), presents annual and seasonal statistics of the NLC observations from places in Europe. The observers of 40 places range in latitude from 51.0°N to 62.5°N, and in longitude from 337.5° to 7.5°. The observations were made in the period 1964-1982. The number of nights where NLC were seen, reached minimum values in 1970 and 1980, the years of maximum solar activity. Maximum numbers of nights with NLC are 33 and 32 in 1967 and 1968 and about 11 years later 50 and 51 in 1977 and 1978 respectively. The anticorrelation between NLC appearance and auroral activity was first analyzed by d'Angelo and Ungstrup (1976) and is again evident in the statistics of Gadsden. A geomagnetic effect in the NLC-appearance could originate from a mesospheric increase of turbulence in disturbed situations within the auroral oval. In addition to the 11 year variability of the NLC occurrence the statistics of Gadsden show that the mean number of nights with NLC is increasing steadily from 20-43 in 1964-1982. The seasonal appearance of NLC is limited to mid May (day 147) to mid August (day 232).

The first analysis of the probability of occurrence of Polar Mesospheric Clouds (PMC) from three seasons (1982-1984) in the north with SME measurements is given in Fig. 6. The mean PMC appearance of the period May 9 (day 128) to August 20 (day 232) increases towards high latitudes. An increase of 40% to 70% probability is obtained from 70° to 80°. The analysis of a complete season in summer 1982 by Thomas (1984) is given in Fig. 7. In this figure the ratio of profiles containing PMC's to the total number within a given latitude band is calculated for three different latitude bands centered at 55°, 65°, and 75°. The curves have an increase of PMC occurrence probability towards high latitude. The maximum of occurrence is in July (day 180-200) with 80% probability at 75°.

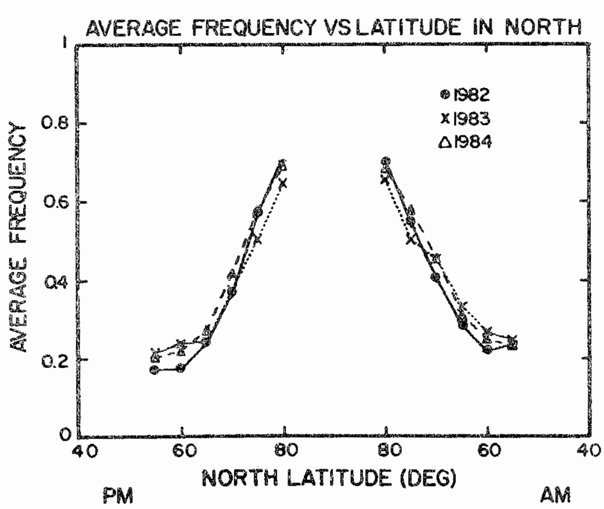

Fig. 6. Average occurrence frequency of PMC determined by the SME UV spectrometer for 3 northern summer seasons. The data have been merged in the interval, 44 days before solstice to 60 days after solstice.

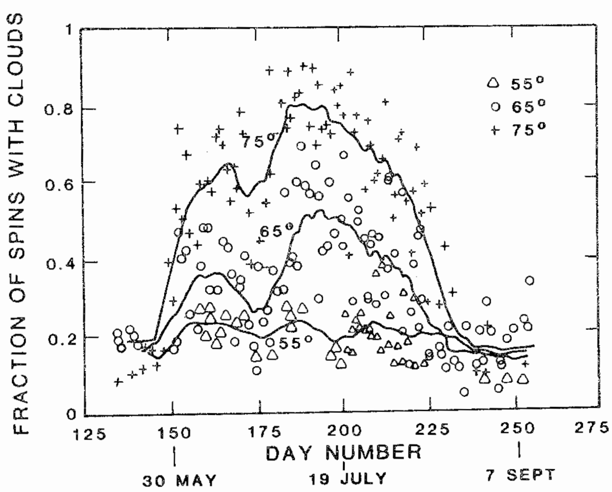

Fig. 7. Fraction of PMC occurrence centred at 55°, 65° and 75° versus day numbers for the 1982 northern summer season. The points are daily averages from six SME satellite orbits. The smooth curves are eleven- day running averages at each latitude of the daily values. (see e.g. Thomas, 1984).

4. OBJECTIVES OF SUPER CAMP

The project Super CAMP is focussed on a study of the structure and dynamics of the middle atmosphere at altitudes 50-150 km above the northern polar region from about 50°N to 80°N during summer 1988. The project Super CAMP will be concentrating on the following scientific goals:

1. To study the effects of dynamics (dissipation of tidal and gravity waves) on the temperature structure, the formation and loss of water ice, the distribution and chemistry of minor constituents (O, O_3, NO, H_2O, odd hydrogen, CO, Na, Ca) including the ionospheric plasma.
2. To measure the water vapor, odd hydrogen and temperature structure and its variability as a function of altitude, latitude, geomagnetic and meteor shower activity.
3. To study tidal and gravity wave dissipation, the structure, horizontal and vertical extention and the life time of turbulent layers of the summer polar mesosphere and the variability with latitude and geomagnetic activity.
4. To study the formation, transport and life time of polar mesospheric clouds and noctilucent clouds, the related densities and size distribution of ice particulates.
5. To study the positive and negative charge of NLC/PMC-water ice particles and the influence on the plasma of the D-region at different latitudes and in different geomagnetic conditions.
6. To intercompare established and new techniques in remote sensing with in situ measurements of atmospheric and ionospheric parameters.

In order to accomplish the main scientific requirements it would be necessary to realize in situ rocket measurements from at least two different ranges, one being located north of the auroral oval, if possible in the region of PMC clouds >75°N. The latitudinal displacement of the rocket ranges will allow

- to study the actual region in the mesosphere where most water ice is formed,
- to investigate the effect of auroral activities on the general circulation, wave dissipation, temperature structure, water ice particles and the density of minor constituents in and outside of the auroral oval,
- to study the transport and formation of water ice within a time scale of 24 hours from two ranges being separated by about 15° in latitude and 25° longitude (Nord, Söndreström in Greenland).

In addition to the latitudinal comparison, the medium and long range differences should be investigated from ranges at similar latitude (Kiruna, Andenes, and Poker Flat). The coordinated sounding rocket measurements from Kiruna and Andenes should lead to a better understanding of the horizontal extention and its displacement, and the life time of thin turbulent layers. The comparison of measurements made in northern Scandinavia and in Poker Flat, Alaska, will allow a study of the possible difference in tidal and gravity wave activity and dissipation.

The project should give new evidences and insights to answer the following outstanding questions on the cold summer mesosphere over the polar cap region:

1. How does the water vapor mixing ratio vary with altitude (60-100 km) and latitude (60°N-80°N)?
2. What is the influence of auroral activity within the auroral oval on the dissipation of gravity and tidal waves and as a consequence on the formation and stability of NLC particles?
3. Is the altitude of zonal wind reversal in the high latitude middle atmosphere dependent on latitude (60°-80°) and geomagnetic activity?
4. Are visible NLC particles formed in the upper mesosphere over the polar cap (>70°N)?
5. Are NLC and PMC ice particles charged, and if so, what is the polarity and what is the effect on the D-region plasma and its composition?
6. Is the mesospheric odd hydrogen density affected by the presence of water ice and what is the result on the chemical loss of atomic oxygen, ozone, carbon monoxide and nitric oxide in the summer polar mesosphere?
7. What are the main sources of turbulence in the summer polar middle atmosphere? Windshears, super adiabatic lapse rates, gravity or tidal wave breaking?
8. What is the horizontal extension and life time of turbulent layers in the summer high latitude middle atmosphere?

For Super CAMP it will be necessary to extend the rocket measurements with experiments operating from ground, airplanes and satellites. These remote sensing experiments should give the required longterm variability of important parameters as temperature, winds, energetic particle flux, density of minor constituents, water ice particle density etc. The possible network of stations around the north pole is shown in Fig. 8. The three rocket ranges outside of the auroral oval are Söndre Strömfjord, Thule and Nord. All three stations are located in Greenland and are accessible by airplanes.

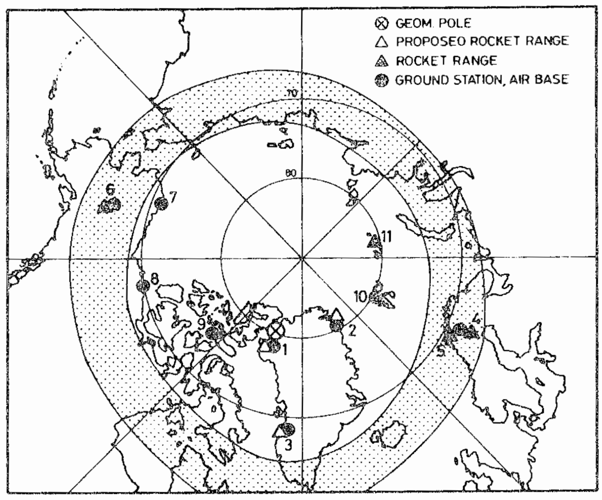

Fig. 8. Proposed stations for Super CAMP for rocket launches (triangle), ground based experiments and airplanes (circles). The different allocations are Thule, Greenland (1), Nord, Greenland (2), Söndre Strömfjord, Greenland (3), Kiruna (Esrange, Eiscat), Sweden (4), Andenes, Norway (5), Poker Flat, Alaska (6), Pt. Barrow, Alaska (7), Cape Perry, Canada (8), Resolute Bay, Canada (9), Spitzbergen (10), Heiss Island, USSR (11). The auroral oval is marked as dotted region.

So far, the stations Thule and Nord have not yet been used for the launching of medium size payloads (Orion, Nike-Orion). The rocket and ground stations are also listed in Table 2 (rocket) and Table 3 (ground). The most ideal combination for a rocket study of the latitudinal variability are Nord at 81.3°N and Söndre Strömfjord at 67°N. The stations are separated by 14.3° in latitude and by 33.1° in longitude, which is ideal for a study of a NLC particle from its origin to its ultimate destination in a visible NLC display. Andenes and Kiruna are well separated in latitude to study displacement and life time of turbulent layers. East-west variability is studied most suitably with a combination between the three rocket places Kiruna/ Andenes, Söndre Strömfjord and Poker Flat. The ground stations south of the NLC and auroral oval would mainly be used for wind and temperature measurements and NLC-observations.

The project Super CAMP would very much gain if the UV-backscatter experiment on the SME-satellite is still operational. Unfortunately, no measurements of mesospheric temperature are now available from satellites; nor will they be available until the U.A.R.S. mission, scheduled for launch in 1989.

Table 2. Available and proposed rocket ranges

RANGE	LAT/LONG	PAY-LOADS	LOCATION
Andenes	69.2/16.0	Large	NLC/Auroral Oval
Kiruna	67.5/21.0	Large	NLC/Auroral Oval
Poker Flat	65.1/309.6	Large	NLC/Auroral Oval
Söndreström	67.0/309.6	Large	PMC/Polar Cap
Heiss Island	80.6/58.1	Small	PMC/Polar Cap
Nord	81.3/342.7	Proposed for large P/L	PMC/Polar Cap
Thule	76.6/291.2	Proposed for large P/L	PMC/Polar Cap

Table 3. Possible Ground Stations for Super CAMP

Location	LAT/LONG	Experiments	Zone
Kiruna	67.8/20.5	Airport, ISR	NLC/Auroral Oval
Andenes	69.3/16.0	MST, LIDAR, OH-T	NLC/Auroral Oval
Ramfjord	69.4/19.0	PRE/ISR	NLC/Auroral Oval
Söndreström	67.0/309.6	ISR	PMC/Polar Cap
College	64.5/211	MST	NLC/Auroral Zone
Poker Flat	64.5/212		
Skibotn	69.3/20.2	LIDAR	NLC/Auroral Oval
Spitzbergen	78.1/15.4	LIDAR/PRR Airport	PMC/Polar Cap
Heiss Island	80.6/58.1	MWR	PMC/Polar Cap
Nord	81.3/342.7	Airport	PMC/Polar Cap
Thule	76.6/342.7	Airport	PMC/Polar Cap
Resolute Bay	74.7/265.1		PMC/Polar Cap
Cape Perry	70.2/235.3		PMC/NLC
Pt. Barrow	71.2/204.5		PMC/NLC
Sheffield/	53.2/358.7	MWR	NLC
Aberdeen	56.0/356.8	MWR	NLC
Collm	51.2/ 13.0	PRE	NLC
Kühlungsborn	54 / 12.7	MWR	NLC
Lindau	52.0/ 12.1	MST	NLC
Saskatoon	52. /253.4	PRE	NLC

5. EXPERIMENTS

The main objectives of Super CAMP require a combination of in situ rocket measurements from at least two rocket launching places at markedly different latitudes together with remote sensing techniques from satellites, airplanes and ground. The parameters to be measured can be grouped in four main categories:

a) Dynamics
b) Composition
c) Aerosol Physics
d) Electrodynamics

All four categories are mutually coupled and a clear allocation of specific measurements to only one of the main fields is not possible. The selection of different experiments should also take into account that one parameter should be measured by different techniques. The experiments and parameters for the four categories are listed in Table 4 (rockets) and Table 5 (ground, airplane and satellite remote sensing). Following a selection of experiments is proposed for measuring the different parameters. The letter added within brackets stands for the experiment application: rockets (R), satellite (S), ground (G), airplane (A), balloon (B).

Table 4. Rocket Experiments

Field	Experiments
Dynamics Turbulence Waves	Ion/Electron Density O-Resonance Fluorescence High Resolution temperature measurements Neutral Mass-Spectrometer Chaff Experiments Release Experiments Occulation Experiments
Composition	Resonance Fluorescence Ion/Neutral Mass Spectrometer IR-Spectrometer, UV-Spectrometer Visible Photometer
Aerosol Physics Nucleation	UV-Light Scattering Mobility/Conductivity Probes Ion/Mass Spectrometer E-Field Experiment DC Ion Probe
Electrodynamic	X-Ray, Precipitating Particle Experiments E-Field Experiments Conductivity Probes Ion/Electron Probes

Table 5. Ground Based, Satellite and Airplane Experiments

Field	Experiment	Parameter
Dynamics	MST-Radar	u, v, w, λ_x, λ_z turbulence
Turbulence	ISR	N_e, T, w
	MWR	u, v
	PRE	u, v, N_e
	LIDAR	T, λ_z
	OH-Interferometer	λ_x, u, v
	NLC-Observation	λ_x, u, v
Composition	Microwave Experiments	H_2O, CO, O_3
Minor Constituents	LIDAR	Na, Ca, Ca^+
	SME-Satellite	O_3, NO, (H_2O in Stratosphere)
Aerosol Physics	SME-Satellite	PMC/NLC particles
Nucleation	NLC-Pictures	NLC display
	LIDAR	NLC particle detection

1. Density: Active falling sphere experiment (R), Lidar (G), Pitot-Tube (R), Optical experiments (R), Passive falling spheres (R).

2. Temperature: Same or similar experiments as in 1), OH-airglow (G), Ion mass spectrometer (R),

3. 3-D-wind: Lidar doppler experiments (G), Active falling sphere (R), Passive falling sphere (R), Release experiments (R), Meteor wind radar (G), OH-Fabry-Perot interferometer (twilight) (G), Partial reflection radar (G), Incoherent scatter radar (G).

4. Turbulence: Electron and ion probes (R), MST-radar (G), Active falling sphere experiments (R), Release experiments (R), Density profiles of atomic oxygen (R).

5. Energy Input: Lyman-α radiation (S,R), Energetic particles (S,R), UV-spectrometer (R), IR-spectrometer (R), Magnetic field variation (G)

6. Atomic Oxygen: Resonance fluorescence (R), Neutral mass spectrometer (R).

7. Ozone: UV-spectrometer (S,R), Microwave sounding (G,A) Ion mass spectrometer (R), 1.27μ photometer (R,S), IR spectrometer (R).

8. Nitric oxide: IR-spectroscopy (R), Ion mass spectrometer (R).

9. Water vapor: IR-photometer (R), Ion mass spectrometer (R), IR-spectrometer (R), Microwave sounding (A). IR-Radiometer (S).

10. CO-density: IR-spectroscopy (R), Microwave sounding (A).

11. Odd Hydrogen: OH-airglow (G), Resonance fluorescence (R), Negative/positive ion mass spectrometer (R). Microwave sounding (H_2O_2) (A,G).

12. Water Ice/Aerosol: UV-scatter experiment (S), Active/passive UV-experiments (R), Ion probes (R), Gerdien probes (R).

13. Electrons: Incoherent scatter radar (G), Partial reflection radar (G), DC-probes (R), Faraday rotation (R,G).

14. Positive ions: Ion mass spectrometer (R), DC-probes (R), Gerdien probes (R).

15. E-Field: DC/AC-probes (R), Release experiments (R), Field mill (R).

16. Particle flux: Particle detectors (R,S), Geomagnetic field (G), X-ray (R,S)

17. Conductivity: Gerdien probes (R).

Various optical and Lidar experiments have difficulties operating in full daylight, but could still be used in Super CAMP if an operation in twilight is possible by selecting the optimum period of operation and geographic location.

6. SPECIAL SCIENTIFIC REQUIREMENTS

6.1 Dynamics

It is essential that primarily ground based techniques should be used to study the transport in the middle atmosphere in three dimensions and the appearance, extension and transport of turbulent layers. MST-Radar, Meteor Wind Radar, Partial Reflection Spaced Antenna Radar, Incoherent Scatter Radar and LIDAR instruments are suitable for this purpose. The ground measurements should be completed with in situ rocket measurements at NLC-latitudes (50-70N) and in the PMC-region (70-80N). Turbulence appears in the summer high latitude mesosphere in thin, horizontally extended layers. The study of such layers with in situ rocket experiments (electron and ion probes, density profiles of O, NO, CO) needs a height resolution of 100 m or better. Furthermore it is expected that the general dynamics of the middle atmosphere over the summer pole varies with latitude. At least one ground station which is located north of the auroral oval would be needed.

6.2 Composition, Minor Constituents

The mesopause of the high latitude middle atmosphere is located around the 90 km altitude in summer and separates very sharply the region above, which is dynamically controlled, from the region below where the life time of minor constituents (O, O_3, NO, CO) is dominated by chemical loss reactions with odd hydrogen species. In the mesosphere the chemical life time of O, O_3, NO and CO seems to be 1-2 orders of magnitude lower compared to the life time of transport by turbulent mixing. The following reaction of O, O_3, NO and CO with odd hydrogen species have to be considered in order to explain the distinct density decrease below the mesopause in the high latitude summer mesosphere:

$$O + OH \rightarrow H + O_2$$
$$O + HO_2 \rightarrow OH + O_2$$
$$O_3 + H \rightarrow OH + O_2$$
$$O_3 + OH \rightarrow HO_2 + O_2$$
$$O_3 + HO_2 \rightarrow OH + 2O_2$$
$$NO + HO_2 \rightarrow OH + NO_2$$
$$CO + OH \rightarrow H + CO_2$$

Previous atomic oxygen density profiles measured by the resonance fluorescence technique give evidence that the mixing ratio of odd hydrogen and water vapor fluctuates with altitude in the summer polar mesosphere. Of special interest is for instance the pronounced atomic oxygen density decrease at the altitude of NLC (81-83 km), an observation which could well be attributed to a local enhancement of the water vapor density and the densities of odd hydrogen species at NLC heights. In situ measurements of minor constituents should have a height resolution of about 1 km or lower, to enable the study of small scale variability of odd hydrogen and water vapor, the influence of turbulent layers on the local mixing of minor constituents.

6.3 Aerosol and NLC-particles

The most suitable instrument for the detection of mesospheric aerosol or water ice particles over the summer polar region are UV-experiments detecting backscatter radiation in different wavelength regions (see e.g. SME UV-backscatter experiment). Such experiments are able to give estimate on the particle size and particle density, the height of NLC and PMC and the variability with latitude and auroral activity. The rocket salvos in Super CAMP could be equipped with a number of small meteorological type rocket payloads with UV-photometers in order to test the presence of NLC or PMC and the related launch conditions for the larger payloads in the salvo. The equipment of the NLC-test rockets could be extended with a positive ion probe of large area, which would give an additional measurement of the presence of NLC or PMC layers.

6.4 Electrodynamics

The charging of NLC water ice particles and its effect on the D-region plasma (conductivity, mobility, electric fields) will need a selection of in situ rocket experiments and corresponding satellite measurements. It is expected that in a sunlit mesosphere NLC and PMC particles would be positively charged, although it is not yet clear if smaller aerosols (meteoric smoke particles) or growing NLC/PMC particles above and below the visible NLC height may carry 1-2 electrons.

Table 6. Number of main experiments

Experiment	NLC (60-70°)	PMC (70-80°)
Medium Payloads:		
Atmospheric Temperature	2	2
Odd Hydrogen, O and Density	2	2
IR-Spectrometer	1	1
Electron/Ion Probes Ion Mass Spectrometer Ionization	2	2
Gerdien Probes, X-Ray, Positive Charge, Electron Density	4	2
E-Fields	2	1
Small Payloads:		
NLC-Location UV-Sensor Positive Charge Probes	6	4
Chaff Release	6	4
Passive Sphere	6	4

7. PERIOD OF OBSERVATION AND NUMBER OF ROCKET PAYLOADS

The Super CAMP experiments should be concentrated in the period of highest occurrence probability of PMC from day 180-210, July 1 to July 31. Towards the end of the observation period an increase of the meteoric particle density is expected from the η-Aquarids.

The rocket ranges to be chosen for Super CAMP should be equipped to launch salvos containing two medium size payloads (Nike-Orion) and two meteorological payloads. The minimum requirement would be the operation from two rocket ranges one at the latitudes of NLC in the auroral oval region and one at higher latitudes well outside of the auroral oval if possible at latitudes 70-80°. In Table 6 the proposed number of experiments to be used in Super CAMP is listed in two categories, 1) medium size payloads, 2) small meteorolgical type pay loads.

8. PLANNING EVENTS

June/July 1985	Questionnaire for experimenters with declaration for an interest in participation, and details on possible instrumentation and the planning on new techniques available in 1988.
August 1985	Information meeting at the IAGA meeting in Prague on the planning and interest to participate in the Super CAMP project.
Dec/Jan 1985/86	Project meeting of Super CAMP in Boulder, Col, or Washington, USA. Formation of Super CAMP working group. Definition phase and proposals to national authorities.
STP 1986	Workshop on the summer polar mesosphere and Working Group Meeting, in Toulouse, France.
Nov/Dec 1986	Project meetings for the rocket and remote sensing experimenters.

9. MAILING LIST BY COUNTRY

AUSTRIA

Friedrich M
Torkar K M

BELGIUM

Ackerman M
Brasseur G
Gerard J C
Simon P C

CANADA

Evans W F J
Gregory J B
Llewellyn E J
Manson A H
Schiff H

DENMARK

Stauning P
Ungstrup E

FEDERAL REPUBLIC OF GERMANY

Arnold F
Czechowsky P
Dahl A F
Ebel A
Fabian P
Grossmann K U
Hartmann G
Krankowsky D
Labitzke K
Lämmerzahl P
Offermann D
Otterbein M
Petzoldt K
Rawer K
Röhrig O
Röttger J
Rose G
Rüster R
Schlegel K
Schmidtke G
Volland H
Widdel U
Wilhelm K
von Zahn U

FRANCE

Bertin F
Blamont J E
Chanin M L
Hauchecorne A
Jegou J P
Megie G
de la Noë J
Thuillier G

GERMAN DEMOCRATIC REPUBLIC

Enzian G
Lauter E A
Taubenheim J

INDIA

Chakrabarty D K
Chakravarty S C
Mitra A P

ITALY

Fiocco G

JAPAN

Hirasawa T
Hirota I
Kato S

NORWAY

Brekke A
Egeland A
Gundersen A
Holtet J A
Thrane E V

SPAIN

Hidalgo M A

SWEDEN

Björn L G
Eiscat
Fredga K
Hultquist B K G
Lundal K
Witt G

SWITZERLAND

Bojkov R D
Eberhardt P
Fröhlich C
Kopp E
Künzi K

UNITED KINGDOM

Barnett J J
Dickinson P H G
Gadsden M
Greer R G H
Houghton J T
Kingsley S P
Müller H G
Smith R W
Thomas L
Rees D
Risbeth H
Rothwell P M
Taylor M J
Wayne R P
Williams E R

UNITED STATES

Anderson J H
Arnoldy R L
Adams G W
Avery S K
Balsley B B
Barth C A
Baker K D
Biondi M A
Bowhill S A
Cahill L J
Donahue T M
Early L
Feldmann P D
Feldman J
Frederick J E
Fritts D C
Forbes J M
Garcia R R
Gardner C S
Garmire
Geller M A
Goldberg R A
Hays P B
Hale L C
Hernandez G
Horvath J J
Kellog P
Kelley M C
Keating G M
Killeen T L
Lindzen R S
Lynch J
Liu C H
Maynard N C
Mauersberger K
Mendillo M
Mentall E J
Meriwether J W
Methews J D
Milliner G
Mozer F
Noxon J F
Olivero J J
Pendleton W R
Philbrick C R
Quiroz R S
Reid G C
Romick C J
Rusch D W
Rapport S
Roper R G
Schmerling E R
Schmidlin F J
Sears R D
Sharp W E
Smith L G
Solomon S
Stair A T
Swider W
Sechrist C F
Shawhan S
Swenson G R
Thomas G E
Thomas R G
Torr D G
Turco R P
Ulwick J C
Watkins B J
Zipf E C

USSR

Avaste O
Danilov A D
Kazimirovksy E S
Rapoport Z Ts
Khodkin S S
Kuminov A A
Pakhomov L V

10. REFERENCES

D'Angelo N and Ungstrup E 1976, On the occurrence of widely observed noctilucent clouds, J. Geophys. Res. 81, 1777.

Balsley B B, Ecklund W L and Fritts D C 1983, VHF echoes from the high latitude mesosphre and lower thermosphere: Observations and interpretations, J. Atmos. Sci. 40, 2451.

Björn L G and Arnold F 1981, Mass spectrometric detection of precondensation nuclei at the arctic summer mesopause, Geophys. Res. Let. 8, 1167.

Björn L G 1984, The cold summer mesopause, Adv. Space Res. 4, Nr. 4, 145.

Björn L G, Kopp E, Herrmann U, Eberhardt P, Dickinson P H, Mackinnon D J, Arnold F, Witt G, Lundin A and Jenkins D B 1985, Heavy ionospheric ions in the formation process of noctilucent clouds, J. Geophys. Res., in press.

Carter D A and Balsley B B 1982, The summer wind field between 80 and 93 km observed by the MST radar at Poker Flat, Alaska (65°N), J. Atmos. Sci. 39, 2905.

Donahue T M, Günther B and Blamont J E 1972, Noctilucent clouds in daytime: Circumpolar particulate layers near the summer mesosphere, J. Atmos. Sci. 30, 515.

Fritts D C, Balsley B B and Ecklund W L 1984, VHF echoes from the arctic mesosphere and lower thermosphere, part II: Interpretation, in book: Dynamics of the middle atmosphere, Ed. J H Holton and T Matsuno, 97-115, D Reidel Publ. Co. Dordrecht.

Gadsden M 1985, Observation of noctilucent clouds from north-west Europe, Ann. Geophys. 3, 119.

Garcia R R and Solomon S 1985, The effect of breaking gravity waves on the dynamics and chemical compositon of the mesosphere and lower thermosphere, J. Geophys, Res., 90, 3850-3868.

Hesstvedt E 1985, Note on nature of noctilucent clouds, J. Geophys. Res. 66, 1161.

Hines C O 1968, A possible source of waves in noctilucent clouds, J. Atmos. Sci. 25, 937.

Jesse O 1896, Die Höhe der leuchtenden Nachtwolken, Ast. Nachrichten, 410, 161.

Kopp E, Eberhardt P, Herrmann U and Björn L G 1985, Positive ion composition of the high latitude summer D-region with noctilucent clouds, J. Geophys. Res., in press.

Murgatroyd R J 1957, Winds and temperatures between 20 km and 100 km - a review, Quart. J. R. Met. Soc. 83, 417.

Murgatroyd R J and Singleton F 1961, Possible meridional circulations in the stratosphere and mesosphere, Quart. J. R. Met. Soc. 87, 125.

Nastrom G D, Balsley B B and Carter D A 1982, Mean meridional winds in the mid- and high-latitude summer mesosphere, Geophys. Res. Let. 9, 139.

Olivero J J and Thomas G E 1985, Climatology of Polar Mesospheric Clouds, J. Atmos. Sci., submitted.

Philbrick C R, Fiare A C and Fryklund D H, 1978 Measurements of atmospheric density at Kwajalein Atoll, 18 May 1977, AFGL-TR-78-0058, Air Force Surveys in Geophysics 384, Air Force Geophysical Laboratory, Hanscom AFB, Ma. 01731, USA.

Philbrick C R, Sipler D P, Balsley B B and Ulwick J C 1984, The STATE experiment-mesospheric dynamics, Adv. Space Res. 4, Nr. 4.

Rüster R 1985, Private communication.

Theon J S, Nordberg W, Katchen L B and Horvarth J J 1967, Some observations on the thermal behavior of the mesosphere, J. Atmos. Sci. 24, 428.

Thomas G E 1984, Solar mesosphere explorer measurements of polar mesospheric clouds (noctilucent clouds), J. Atmos. Terr. Phys. 46, 819.

Thomas G E and McKay Ch P 1985, On the mean particle size and water content of polar mesospheric clouds, Planet. Space Sci., in press.

Turco R P, Toon O B, Whitten R C, Keesee R G, and Hollenbach D 1982, Noctilucent clouds: Simulation studies of their genesis, properties and global influences, Planet. Space Sci. 30, 1147.